Intramolecular Proton Transfer from Multiple Sites in Catalysis by Murine Carbonic Anhydrase V†

J. Nicole Earnhardt,§ Minzhang Qian,‡ Chingkuang Tu,‡ Philip J. Laipis,§ and David N. Silverman*,§,‡

Department of Biochemistry and Molecular Biology and Department of Pharmacology and Therapeutics, University of Florida College of Medicine, Gainesville, Florida 32610-0267

Received December 1, 1997; Revised Manuscript Received February 25, 1998

ABSTRACT: The hydration of CO_2 catalyzed by carbonic anhydrase requires proton transfer from the zinc-bound water at the active site to solution for each cycle of catalysis. In the most efficient of the mammalian carbonic anhydrases, isozyme II, this transfer is facilitated by a proton shuttle residue, His 64. Murine carbonic anhydrase V (mCA V) has a sterically constrained tyrosine at the analogous position; it is not an effective proton shuttle, yet catalysis by this isozyme still achieves a maximal turnover in CO_2 hydration of 3×10^5 s^{-1} at pH > 9. We have investigated the source of proton transfer in a truncated form of mCA V and identified several basic residues, including Lys 91 and Tyr 131, located near the mouth of the active-site cavity that contribute to proton transfer. Intramolecular proton-transfer rates between these shuttle groups and the zinc-bound water were estimated as the rate-determining step in k_{cat} for hydration of CO_2 measured by stopped-flow spectrophotometry and in the exchange of ^{18}O between CO_2 and water measured by mass spectrometry. Comparison of k_{cat} in catalysis by Lys 91 and Tyr 131 and the corresponding double mutant showed a strong antagonistic interaction between these sites, suggesting a cooperative behavior in facilitating the proton-transfer step of catalysis. Replacing four potential proton shuttle residues produced a multiple mutant that had 10% of the catalytic turnover k_{cat} of the wild type, suggesting that the main proton shuttles have been accounted for in mCA V. These replacements caused relatively small changes in k_{cat}/K_m for hydration, which measures the interconversion of CO_2 and HCO_3^- in a stage of catalysis that is separate and distinct from the proton transfers; these measurements serve as a control indicating that the replacements of proton shuttles have not caused structural changes that affect reactivity at the zinc.

Carbonic anhydrase V (CA V)[1] is a mitochondrial enzyme found predominantly in liver; it is a member of the α class of carbonic anhydrases that includes the mammalian isozymes (reviewed in ref *1*). The catalytic properties of murine carbonic anhydrase V (mCA V) have been characterized (*2*), and its crystal structure is determined to 2.45-Å resolution (*3*). Similar to the other carbonic anhydrases of the α class, mCA V is a monomeric zinc metalloenzyme of molecular mass near 30 kDa that catalyzes the hydration of carbon dioxide to form bicarbonate and a proton. The catalytic pathway of mCA V is similar to that of the well-studied CA II in many respects. The first stage of catalysis comprises the hydration of CO_2 involving the zinc-bound hydroxide to yield bicarbonate; the departure of bicarbonate leaves a water bound to the zinc (eq 1). The second stage requires a proton to be transferred from zinc-bound water to buffer in solution (designated as B in eq 2) to regenerate the zinc-bound hydroxide (*4*). For CA II, this proton-transfer proceeds through an intramolecular proton shuttle (designated in eq 2 as H^+ to the left of E), which subsequently releases the proton to solution. In CA II, this intramolecular proton shuttle has been identified as His 64 (*5*, *6*), which extends into the active-site cavity with the Nδ of its imidazole ring 7.4 Å from the zinc and with no apparent interactions with other residues (*7*).

$$CO_2 + EZnOH^- \rightleftarrows EZnHCO_3^- \overset{+H_2O}{\rightleftharpoons} HCO_3^- + EZnH_2O \quad (1)$$

$$EZnH_2O + B \rightleftarrows H^+EZnOH^- + B \rightleftarrows EZnOH^- + BH^+ \quad (2)$$

mCA V has a tyrosine residue at position 64 that is not an efficient proton shuttle (*2*). However, it is possible to activate mCA V by placing a histidine residue at position 64 along with other changes in the active site (*8*). Studies using isotope effects, pH dependencies, and chemical rescue have shown that these intramolecular proton-transfer steps are rate-determining for maximal velocity (*6*, *9*).

† This work was supported by Grant GM25154 from the National Institutes of Health.

§ Department of Biochemistry and Molecular Biology.

‡ Department of Pharmacology and Therapeutics.

* Address correspondence to this author. Telephone: (352) 392-3556; fax: (352) 392-9696; e-mail: silvrmn@nervm.nerdc.ufl.edu.

[1] Abbreviations: CA, carbonic anhydrase; mCA V, murine CA V; HCA II, human carbonic anhydrase II; Y64A, the mutant with Tyr 64 replaced by Ala; Mes, 2-(*N*-morpholino)ethanesulfonic acid; Mops, 3-(*N*-morpholino)propanesulfonic acid; Hepes, *N*-(2-hydroxyethyl)-piperazine-*N*′-2-ethanesulfonic acid; Taps, 3-[[tris(hydroxymethyl)-methyl]amino]propanesulfonic acid; Ches, 2-(cyclohexylamino)ethane-sulfonic acid; Tris, tris(hydroxymethyl)aminomethane; Ted, 1,4-diazabicyclo[2.2.2]octane or triethylenediamine; SHIE, solvent hydrogen isotope effect.

S0006-2960(97)02920-6 CCC: $15.00
Published on Web 04/28/1998

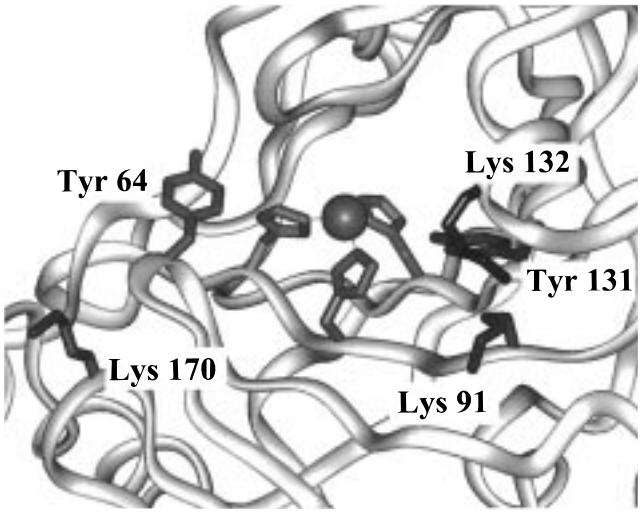

FIGURE 1: Location of ionizable residues near the active site cavity of murine carbonic anhydrase V from the crystal structure of Boriack-Sjodin et al. (*3*). The three ligands of the zinc are His 94, 96, and 119.

Position 64 in carbonic anhydrase is not the only site from which proton transfer can occur. Liang et al. (*10*) placed a histidine residue at four other positions within the active-site cavity of isozyme II and found that a His at 67 was capable of enhancing catalytic activity but at a level no greater than 20% of the wild-type enzyme. Ren et al. (*11*) showed that His 67 in human CA III is capable of proton transfer, but again it is not as efficient as His 64 in CA III. It is significant that the mutants of carbonic anhydrase lacking a histidine proton shuttle in the active-site cavity can still sustain a catalytic turnover k_{cat} for hydration at pH near 9 of 10^4 s^{-1} as for human CA III (*12*) and as great as 3×10^5 s^{-1} for mCA V (*2*). This suggests the presence of one or more basic residues that act as proton shuttles.

Since mCA V supports catalysis at a rapid rate at high pH but is lacking His 64 as a prominent proton shuttle, it is pertinent to ask what residues in mCA V support this significant activity. There are a number of lysine and tyrosine residues in mCA V located in the active-site cavity or around its rim. In this study, these residues have been replaced with alanine, and the initial velocities in catalysis by the resulting mutants were measured using stopped-flow spectrophotometry; catalysis of ^{18}O exchange between CO_2 and water was also measured using mass spectrometry. The results show that the catalytic activity in mCA V is supported by multiple proton transfers involving a number of ionizable groups of basic pK_a, some more distant from the zinc than residue 64. Although there is no single prominent proton shuttle, Lys 91 and Tyr 131 with their amino and phenolic hydroxyl groups 14.4 and 9.1 Å from the zinc (*3*), as shown in Figure 1, account for about half of the catalytic turnover. Moreover, the interaction between these proton shuttles in catalysis is not simply additive but antagonistic, reflecting their adjacent location and suggesting a cooperative behavior in facilitating the proton-transfer step of catalysis. Replacing four of these possible proton shuttle residues produced a multiple mutant that has 10% of the catalytic turnover k_{cat} of the wild type, suggesting that the main proton shuttles have been accounted for in mCA V. As a control, we have determined that these replacements cause relatively small changes in k_{cat}/K_m for hydration, which measures the interconversion of CO_2 and HCO_3^- in a stage of catalysis that is separate and distinct from the proton transfers.

EXPERIMENTAL PROCEDURES

Site-Specific Mutagenesis. The coding sequence of mouse CA V was derived from BALB/C mouse liver mRNA by reverse transcription and PCR (*2*, *8*). Mutant forms of mCA V were created using a mutating oligonucleotide (*13*) in the pET31 expression vector system (*14*); alterations were verified by DNA sequencing.

Expression and Purification. Wild-type and mutant forms of the enzyme were expressed from the pET vector after transformation into *Escherichia coli* BL21(DE3)pLysS (*15*). All of the expressed enzymes were truncated forms lacking the first 51 amino terminal residues. In a sequence numbering scheme consistent with CA II, the expressed mCA V variants began at residue 22, Ser. This truncated form of mCA V (denoted mCA Vc by Heck et al.; *2*) has been shown to have identical catalytic properties to mCA V expressed from both a full-length coding sequence and a 30-residue truncation of mCA V (*2*).

Purification was performed through previously described procedures with slight modifications (*2*). Frozen cells containing expressed recombinant mCA V mutants were thawed in a solution of 25 mM Tris, pH 8.5, containing 2 mM EDTA, 0.2 mM phenylmethanesulfonyl fluoride, 5 mM benzamidine, 0.4 mM $MgCl_2$, 0.4 mM $ZnSO_4$, 0.1% β-mercaptoethanol, 0.1 mg/mL deoxyribonuclease I, and 0.5 mg/mL lysozyme with stirring for 2 h in 4 °C. After cell lysis, the cell debris was pelleted by centrifugation at 43000*g* for 30 min at 4 °C. The supernatant was added to an ultro gel filtration column. The protein eluate was then subjected to affinity chromatography on a gel containing *p*-aminomethylbenzenesulfonamide coupled to agarose beads as described by Khalifah et al. (*16*). Electrophoresis on a 10% polyacrylamide gel stained with Coomassie Blue revealed the purity of the enzyme samples, and all enzyme samples used in the kinetic experiments were greater than 95% pure. Active mCA V mutant enzyme concentration was determined by inhibitor titration of the active site with ethoxzolamide by measuring ^{18}O exchange between CO_2 and water (see below). The enzyme was then stored at 4 °C.

Initial Velocities. Stopped-flow spectrophotometry measurements were carried out by the method described by Khalifah (*17*). Initial velocities were determined by following the change in absorbance of a pH indicator at 25 °C using a stopped-flow spectrophotometer (Applied Photophysics Model SF.17MV). CO_2 solutions were made by bubbling carbon dioxide into water or D_2O for the solvent hydrogen isotope effect studies. The maximum concentration of CO_2 in H_2O achieved by this method was 17 mM following dilution. Dilutions were made through two syringes with a gastight connection, the CO_2 concentrations for the substrates ranged from 0.7 to 17 mM. Final buffer concentrations were 25 mM, and each solution contained Na_2SO_4 to achieve a final ionic strength of 0.2 M. The buffer−indicator pairs, pK_a values, and the wavelengths observed are as follows: Mes (pK_a = 6.1) and chlorophenol red (pK_a = 6.3) 574 nm; Mops (pK_a = 7.2) and *p*-nitrophenol (pK_a = 7.1) 400 nm; Hepes (pK_a = 7.5) and phenol red (pK_a = 7.5) 557 nm; 1,2-dimethylimidazole (pK_a = 8.2) and *m*-cresol

Table 1: Maximal Values of k_{cat}/K_m and k_{cat} for CO_2 Hydration and k_B with pK_a Values Obtained from Their pH Profiles for Wild-Type and Mutants of Murine Carbonic Anhydrase V[a]

	k_{cat}/K_m (μM^{-1} s^{-1})	p$K_{a(k_{cat}/K_m)}$	k_{cat} (ms^{-1})	p$K_{a(k_{cat})}$	k_B (ms^{-1})	p$K_{a(kB)}$
Y64A	19 ± 1[c]	7.8 ± 0.1[c]	250 ± 50[c]	9.2 ± 0.1[c]	80 ± 10	8.7 ± 0.3
Y64A/Y131A	22 ± 1[c]	7.4 ± 0.1[c]	80 ± 10[c]	8.8 ± 0.1[c]	30 ± 10	>8.7
Y64A/K91A/Y131A	21 ± 1	7.6 ± 0.1	70 ± 10	9.1 ± 0.1	20 ± 10	>8.5
wild type	35 ± 1[b]	7.4 ± 0.1[b]	320 ± 30[b]	9.2 ± 0.2[b]	120 ± 20	8.6 ± 0.1
K91A	34 ± 1	7.5 ± 0.1	130 ± 10	9.0 ± 0.1	30 ± 10	8.9 ± 0.2
Y131A	37 ± 1[c]	7.1 ± 0.1[c]	180 ± 20[c]	9.2 ± 0.1[c]	110 ± 10	>8.5
K91A/Y131A	36 ± 16[d]	7.9 ± 0.4	150 ± 30	9.1 ± 0.2	70 ± 10	8.3 ± 0.2
	18 ± 17[d]	6.9 ± 0.4				
K132A	55 ± 1	7.2 ± 0.1	270 ± 20	9.1 ± 0.1	110 ± 20	8.3 ± 0.1
K170A	56 ± 2	7.3 ± 0.1	270 ± 20	8.9 ± 0.1	140 ± 130	>8.5
Y64A/K91A/Y131A/K132A	60 ± 2	7.6 ± 0.1	32 ± 6	9.1 ± 0.1	60 ± 10	8.5 ± 0.2

[a] Maximal values of k_{cat}/K_m and k_B were determined from pH profiles for the exchange of ^{18}O measured by mass spectrometry, and the maximal values of k_{cat} were determined from pH profiles of the hydration of CO_2 obtained by stopped-flow spectrophotometry. [b] Data taken from Heck et al. (*2*). [c] Data taken from Heck et al. (*8*). [d] These standard errors representing the fits to ionization curves are much larger than for the other data due to the similar values of the apparent pK_a.

purple (pK_a = 8.3) 578 nm; Taps (pK_a = 8.4) and *m*-cresol purple (pK_a = 8.3) 578 nm; Ches (pK_a = 9.3) and thymol blue (pK_a = 8.9) 596 nm; Ted (pK_a = 9.2) and thymol blue (pK_a = 8.9) 596 nm. For each substrate at each pH, the mean initial velocity was determined with at least five traces of the initial 5−10% of the reaction. The uncatalyzed rates were determined in a similar manner and subtracted from the total observed rates. The kinetic constants k_{cat} and k_{cat}/K_m were determined by a nonlinear least-squares method using Enzfitter (Elsevier-Biosoft).

^{18}O Exchange. Using an Extrel EXM-200 mass spectrometer utilizing a membrane permeable to gases, we measured the rate of exchange of ^{18}O between species of CO_2 and water and the rate of exchange of ^{18}O into solvent water as $H_2{}^{18}O$ catalyzed by the carbonic anhydrases (eqs 3 and 4) (*18*). No buffers were added except where indicated, and a total ionic strength of 0.2 M was maintained with Na_2SO_4 at 25 °C.

$$HCOO^{18}O^- + EZnH_2O \rightleftarrows EZnHCOO^{18}O^- \rightleftarrows COO + EZnO^{18}H^- \quad (3)$$

$$EZnO^{18}H^- + BH^+ \rightleftarrows H^+EZn^{18}OH^- + B \rightleftarrows EZnH_2{}^{18}O \xrightarrow{+H_2O} EZnH_2O + H_2{}^{18}O \quad (4)$$

From these experiments, two rates are determined, one of which is the rate of the catalytic interconversion of CO_2 and HCO_3^- (eq 3) at chemical equilibrium, R_1. The substrate dependence of R_1 is described by eq 5.

$$R_1/[E] = k_{cat}{}^{ex}[S]/(K_{eff}{}^{s} + [S]) \quad (5)$$

[E] is the total enzyme concentration, $k_{cat}{}^{ex}$ is the rate constant for maximal interconversion of CO_2 and HCO_3^-, $K_{eff}{}^{s}$ is the apparent substrate binding constant, and [S] is the concentration of substrate CO_2 and/or HCO_3^- (*19*). The ratio $k_{cat}{}^{ex}/K_{eff}{}^{s}$ was determined from R_1 when $[S] \ll K_{eff}{}^{s}$ or from varying substrate concentrations. In theory and in practice when $[CO_2] \ll K_{eff}{}^{CO_2}$, then $k_{cat}{}^{ex}/K_{eff}{}^{CO_2}$ is equal to k_{cat}/K_m for CO_2 hydration.

The second parameter is the rate of release of $H_2{}^{18}O$ from the enzyme into solvent water as $H_2{}^{16}O$ (eq 4). This rate depends on concentrations of the shuttle residue in the protonated state and of the zinc-bound hydroxide. Equation 6 represents $R_{H_2O}/[E]$ in terms of the appropriate ionization constants and k_B, the rate constant for intramolecular proton transfer from the shuttle group to the zinc-bound hydroxide.

$$R_{H_2O}/[E] = k_B/\{(1 + K_B/[H^+])(1 + [H^+]/K_E)\} \quad (6)$$

K_B is the ionization constant for the donor group, and K_E is the ionization constant of the zinc-bound water.

In the measurement of solvent hydrogen isotope effects, we determined kinetic constants using solutions of 99.8% D_2O. All pH and pD measurements are uncorrected pH meter readings.

RESULTS

The mutants constructed for this study have the potential proton-transfer residues at positions 64, 91, 131, 132, and 170 replaced with alanine in single and multiple mutations (Figure 1, Table 1). The pH profiles for k_{cat}/K_m for hydration of CO_2, determined from ^{18}O exchange rates, varied as if dependent on the base form of a single ionizable group (Figure 2) with apparent values of pK_a that were similar for each mutant, from pK_a 7.1 to pK_a 7.9 (Table 1). The double mutant K91A/Y131A mCA V was an exception in that two ionizations fit the data better than one; however, the apparent values of pK_a were very similar for the two ionizations (Table 1). The alanine replacements did not cause large changes in the maximal values of k_{cat}/K_m, which had magnitudes ranging from 1.9 to 6.0 × 10^7 M^{-1} s^{-1} for all of the mutants studied (Table 1). The magnitudes of k_{cat}/K_m appeared to occur in three groups as shown in Table 1; for example, the mutants containing Tyr 64 including wild-type mCA V have values of k_{cat}/K_m very near 3.5 × 10^7 M^{-1} s^{-1}, and the mutants containing Ala 64 have values very near 2.0 × 10^7 M^{-1} s^{-1} (Table 1). The ratio k_{cat}/K_m contains rate constants for the conversion of CO_2 into HCO_3^- up to and including the first irreversible step, the departure of HCO_3^- (eq 1). Therefore, these mutants are not causing significant changes in this stage of catalysis or influencing the surrounding environment of the zinc-bound water in a manner that would alter its pK_a or catalytic activity.

Measurement by stopped flow of the steady-state constants k_{cat} for CO_2 hydration had a pH dependence that could also

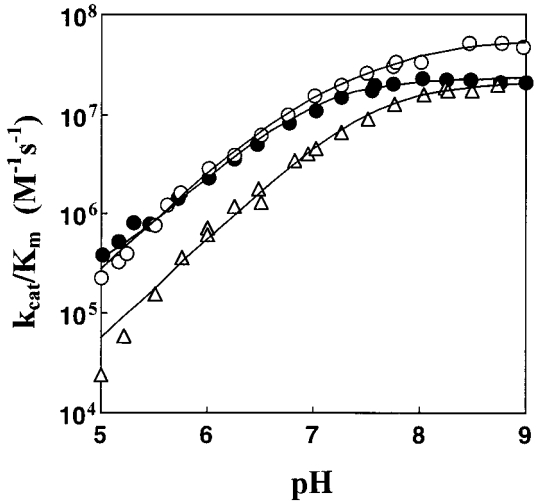

FIGURE 2: pH dependence of k_{cat}/K_m for hydration of CO_2 determined by ^{18}O exchange catalyzed by (●) wild-type mCA V (Heck et al.; *2*), (○) K91A/Y131A mCA V, and (△) Y64A/K91A/Y131A mCA V at 25 °C. Total ionic strength was maintained at 0.2 M by addition of Na_2SO_4; no buffers were used. Lines are a nonlinear least-squares fit to a single ionization for wild type and Y64A/K91A/Y131A and to two ionizations for the K91A/Y131A mutant resulting in the parameters given in Table 1.

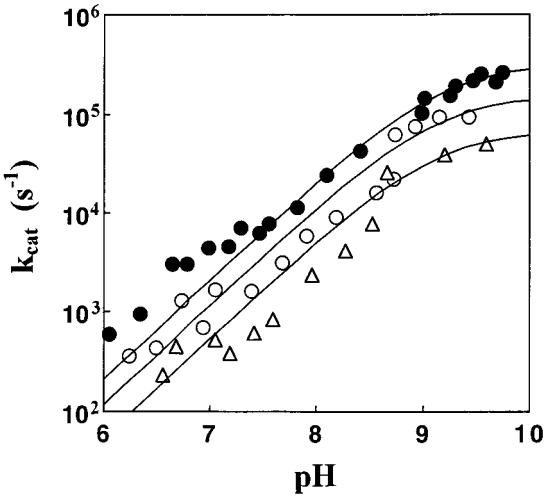

FIGURE 3: pH dependence of k_{cat} for hydration of CO_2 determined by stopped-flow spectrophotometry catalyzed by (●) wild type (Heck et al.; *2*); (○) K91A/Y131A mCA V; and (△) Y64A/K91A/Y131A mCA V at 25 °C. Total ionic strength was maintained at 0.2 M by addition of Na_2SO_4. Lines are a nonlinear least-squares fit to a single ionization resulting in the parameters given in Table 1.

be fit to a single ionization with apparent values of pK_a in the narrow range of 8.8−9.2 for wild type and mutants (Table 1) with typical data shown in Figure 3. The variation in the maximal values of k_{cat} ranged from 3.2×10^5 s^{-1} for the wild-type enzyme to 0.32×10^5 s^{-1} for the multiple mutant Y64A/K91A/Y131A/K132A (Table 1).

The ^{18}O exchange rate constant $R_{H_2O}/[E]$ describes the rate of release of $H_2{}^{18}O$ from the enzyme into solvent water at chemical equilibrium and involves proton transfer to the zinc-bound hydroxide in the dehydration direction (eq 4). The pH profiles of $R_{H_2O}/[E]$ were typically bell-shaped for the mutants of Table 1 and yielded a rate constant k_B for intramolecular proton transfer and values of pK_a for the zinc-bound water and for the intramolecular proton donor determined by least-squares fitting of eq 6 to the pH profiles

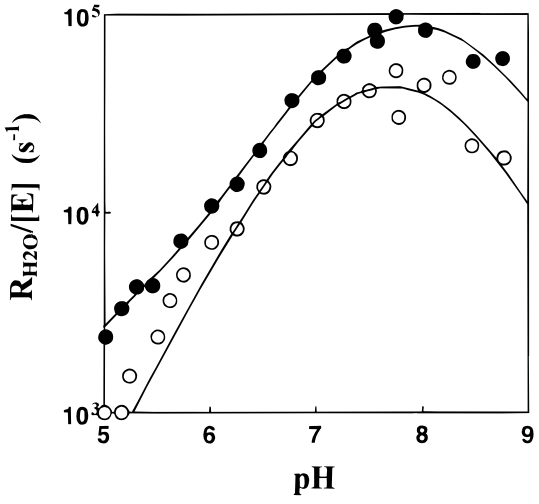

FIGURE 4: pH dependence of $R_{H_2O}/[E]$, the rate constant for release from the enzyme, catalyzed by (●) wild-type mCA V and (○) the mutant K91A/Y131A mCA V at 25 °C. The total concentration of all species of CO_2 was 25 mM, the total ionic strength of solution was maintained at 0.2 M by addition of Na_2SO_4, and no buffers were added.

of $R_{H_2O}/[E]$. The values of the pK_a of the zinc-bound water were in agreement, within 0.1 or 0.2 unit, with those obtained from the pH profiles of k_{cat}/K_m. Application of these procedures to typical data are shown in Figure 4 for wild-type mCA V and K91A/Y131A mCA V. The ^{18}O exchange results again show a narrow range of values for the proton donor of pK_a from 8.3 to 8.9 (Table 1). These values confirm the pK_a near 9 found from the pH profile of k_{cat} for the proton shuttle also shown in Table 1. The wild-type enzyme had the largest value of the rate constant k_B for intramolecular proton transfer with the smallest value being observed for the triple mutant Y64A/K91A/Y131A at 17% of the wild type (Table 1). The magnitudes of k_B and k_{cat} can only be compared qualitatively since they represent proton transfer in the dehydration and hydration directions.

The solvent hydrogen isotope effect (SHIE) observed for catalysis of CO_2 hydration by Y64A/K91A/Y131A mCA V was 1.4 ± 0.2 for k_{cat}/K_m at pH 9.2. This is consistent with no rate-contributing proton transfer in the interconversion of CO_2 and HCO_3^- (eq 1). The SHIE at pH 9.2 on k_{cat} was 4.1 ± 0.5, consistent with rate-determining proton transfer involving the aqueous ligand of the zinc (eq 2).

We also measured the capacity of mutants of mCA V to be enhanced in catalysis by proton donors or acceptors from solution through chemical rescue. These experiments were done using the buffers of small size, imidazole and 1,2-dimethylimidazole, and one of bulky molecular size, Ted. It was found that imidazole was able to activate $R_{H_2O}/[E]$ catalyzed by Y64A/F65A mCA V in a saturable manner with an apparent K_m for this buffer near 91 mM at pH 6.3 (Figure 5). Imidazole had a slight inhibitory effect on $R_1/[E]$ and on k_{cat}/K_m causing these values to decrease with an apparent K_i of 0.40 ± 0.17 M upon increasing imidazole up to a concentration of 200 mM (Figure 5). The maximal value of $R_{H_2O}/[E]$ when corrected for this inhibition was estimated at $(1.1 \pm 0.2) \times 10^5$ s^{-1}; this is identical to the value of 1×10^5 s^{-1} for Y64H/F65A mCA V in the absence of buffer at pH 6.3 (with total substrate and ionic strength as described in Figure 5).

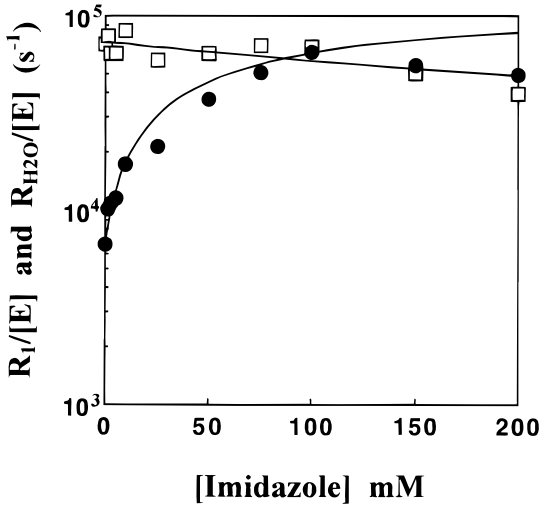

FIGURE 5: Dependence of R_{H_2O}/[E] (●) and R_1/[E] (□) as a function of the concentration of imidazole at pH 6.3 and 25 °C. The total concentration of all species of CO_2 was 25 mM, and the total ionic strength of solution was maintained at a minimum of 0.2 M by addition of Na_2SO_4. The data for R_{H_2O}/[E] approach a maximal value of $(1.1 \pm 0.2) \times 10^5$ s^{-1} when corrected for the apparent inhibition manifested in R_1/[E].

Ted and 1,2-dimethylimidazole caused no change in k_{cat}/K_m catalyzed by Y64A/K91A/Y131A mCA V at concentrations up to 200 mM. R_{H_2O}/[E] catalyzed by this triple mutant was 8.9×10^3 s^{-1} with no buffer and increased in a saturable manner to values approaching a maximum of $(1.8 \pm 0.3) \times 10^4$ s^{-1} with an apparent K_m of 130 mM upon addition of 1,2-dimethylimidazole (pH 8.2, 25 °C, ionic strength maintained at a minimum 0.2 by addition of Na_2SO_4). This maximum is very similar to the value of 2.2×10^4 s^{-1} measured under the same conditions but in the absence of buffers with Y64H/F65A mCA V. The following similar observation was made by stopped flow measuring initial velocities. The estimated values of k_{cat} for CO_2 hydration catalyzed by 1.2 μM Y64A/K91A/Y131A mCA V increased from a value close to 1×10^3 s^{-1} to values approaching $(1.0 \pm 0.3) \times 10^5$ s^{-1} with an apparent K_m of 80 mM as concentrations of 1,2-dimethylimidazole increased from 1 to 200 mM (pH 8.2, 25 °C, ionic strength maintained at a minimum of 0.2 M). Again, this is close to the value of k_{cat} $(2.0 \pm 0.4) \times 10^5$ s^{-1} under these conditions for Y64H/F65A mCA V (8). The buffer Ted (at pH 9.3 and 25 °C) up to concentrations of 100 mM caused no change in R_{H_2O}/[E] catalyzed by the triple mutant; however, Ted at these concentrations did cause an increase of greater than 10-fold with a value of K_m of 70 mM in the initial velocity of CO_2 hydration.

DISCUSSION

In mCA V, we seek to identify the residue or residues of pK_a near 9 that act as proton acceptors in the hydration direction of catalysis. For this purpose, the proton-transfer capacity was investigated for a number of lysine and tyrosine residues in the active-site cavity and near its rim. Five potential proton shuttle residues in the active-site cavity or near its mouth in mCA V were replaced; this includes many evident basic groups in the vicinity of the active site that could participate as proton shuttles. These have been replaced by alanine and the effect on k_{cat} for hydration and on ^{18}O exchange have been measured.

Role of Proton Shuttles. Among the variants of mCA V in Table 1, wild-type mCA V has the largest value of k_{cat}, and the various single mutants with potential proton shuttles replaced have lower values. A similar observation is also made for k_B, a rate constant for intramolecular proton transfer determined from ^{18}O exchange, in which again the wild-type enzyme has the largest value (Table 1). These decreases in k_{cat} for hydration and k_B observed in our mutants of mCA V are interpreted as decreased efficiency of the intramolecular proton-transfer processes. This interpretation is supported by the following considerations. A wide body of previous data indicates that k_{cat} for catalysis by carbonic anhydrase is dominated by intramolecular proton transfer between the zinc-bound water and proton shuttle residues (*4*−*6*), and the studies with murine CA V are also consistent with such rate-determining steps for k_{cat} (*2*, *8*). Many of the previous experiments to confirm rate-limiting proton transfer in this catalysis have been repeated in this study with one of the least active mutants and other mutants of Table 1: Y64A/K91A/Y131A has a solvent hydrogen isotope effect of 4.1 on k_{cat} for hydration; k_{cat} is activated by proton donors in solution, an example of chemical rescue; and k_{cat} and R_{H_2O} have pH profiles that are consistent with intramolecular proton transfer.

There is no single replacement in Table 1 that causes a decrease in k_{cat} or k_B as large as the 40-fold decrease that resulted from the replacement of His 64 by Ala in HCA II (*6*). Thus, it appears that in mCA V there is not one predominant proton shuttle group as in HCA II but many shuttle groups. The closest potential side chain among those we studied is Tyr 64 with its hydroxyl oxygen 7.7 Å from the zinc. However, this side chain is pointing away from the zinc in the crystal structure and appears limited in its mobility by the adjacent Phe 65, which most likely accounts for the very slight reduction (or no change, Table 1) when it is replaced by alanine (*2*, *8*). Among the remaining lysines and tyrosines of Table 1, the closest to the zinc are Tyr 131 with its hydroxyl oxygen 9 Å from the zinc and Lys 91 with its Nζ 14 Å from the zinc (*3*). Accordingly, these replacements among the single mutants caused the largest decreases in k_{cat} (Table 1). The residues Lys 132 and Lys 170 have their Nζ a distance of 19 and 20 Å, respectively, from the zinc; the decreases in k_{cat} when these residues are replaced by Ala are very small (or no change) as compared with k_{cat} for wild type (Table 1).

The rate constants for intramolecular proton-transfer k_B determined by ^{18}O exchange measure proton transfer in the dehydration direction and are different from the values of k_{cat} for hydration discussed above. The values of k_B add an important component to our considerations since they represent data taken in the absence of buffer and, unlike k_{cat} measured at steady-state, do not contain the possibility of direct proton transfer between the buffer and the zinc-bound water. The decreases in k_B for the mutants of Table 1 as compared with wild type in general mirror the decreases in k_{cat}. However there are notable exceptions, such as for Y131A which has a rather greater effect on k_{cat} than on k_B as compared with wild type (Table 1). On the other hand, K91A has a greater effect on k_B. No additional evidence is available to explain these observations.

Hence, among the replacements of basic groups in Table 1 resulting in single mutants, the replacements of Lys 91 and Tyr 131 caused significant decreases in k_{cat} for hydration. This evidence is consistent with proton shuttle roles for Lys 91 and Tyr 131 as they participate in the intramolecular proton transfer steps. There are other explanations for these observations, but they can be considered less likely. For example, it is possible that these residues are not proton shuttles themselves but are residues that contribute to proton transfer by their effects on the formation of hydrogen-bonded water networks in the active-site cavity. The following observations indicate that changes in catalysis by the mutants of Table 1 are not significantly affected by any changes in such water structure.

First, the lack of a significant effect of the replacement of the suggested proton-transfer residues (K91, Y131) on k_{cat}/K_m (Table 1) as compared to wild type suggests that the chemistry of CO_2 hydration at the zinc is not affected by replacements at these distant sites, possibly including changes in water structure. However, this approach needs further support since studies of human CA II have shown that the insertion of bulky residues including Phe at position 65 adjacent to the proton shuttle residue His 64 alters water structure in the active site of the crystal structure, an effect that is accompanied by significant decreases in k_{cat} with smaller or no changes in k_{cat}/K_m (*20*, *21*). The crystal structures of mCA V and human CA II are very similar with backbone conformations that are superimposable with a rms deviation of 0.93 Å (*3*). When the substitution Phe 65 → Ala is made in mCA V, a decrease in k_{cat} is not observed for the resulting F65A as compared with wild type (Table 1 in ref *8*). This suggests that the proton-transfer dependent values of k_{cat} for mCA V, presumably involving proton transfer from more distant sites, are not affected by changes in water structure caused by the replacement Phe 65 → Ala.

Another observation suggesting that changes in water structure are not significantly involved in the data of Table 1 is that chemical rescue of certain of these mutants of mCA V with imidazole or 1,2-dimethylimidazole activates catalysis to levels found for the mutant Y64H/F65A containing an unhindered imidazole as proton shuttle (*8*). Thus, the mutant Y64A/F65A when enhanced with imidazole achieved values of R_{H_2O}/[E] near 1×10^5 s^{-1} (Figure 5) identical to that of Y64H/F65A. Similarly, the mutant Y64A/K91A/Y131A was activated by 1,2-dimethylimidazole to levels of R_{H_2O}/[E] and k_{cat} for hydration similar to that of Y64H/F65A in the absence of this buffer (or at very low buffer concentration). These observations also suggest that substitution of K91 and Y131 on the periphery of the active-site cavity has no measurable effect on proton transfer and presumably water structure when the proton shuttle is 1,2-dimethylimidazole.

Although Table 1 reports decreased catalysis upon replacement of Tyr 131 with Ala, there is the following evidence that proton transfer to enhance catalysis can occur from position 131. Chemical modification of Y131C mCA V with 4-chloromethylimidazole and 4-bromoethylimidazole caused up to 3-fold enhancement of R_{H_2O}/[E] at pH < 7 with pH profiles consistent with the presence of a proton donor of pK_a near 6.[2] These results indicate that the imidazole group of the chemically modified Cys 131 promotes proton transfer and shows that a proton shuttle at this site can act as a proton donor in catalysis. Attempts to observe an enhancement of catalysis with Y131H were not conclusive.

Experiments were performed to eliminate some additional considerations as contributing to proton transfer, showing they have no significant effect on k_{cat}. For example, rate constants for the initial velocities of catalysis do not increase with an increase of enzyme concentration (data not shown). Thus, there is no significant intermolecular proton transfer involving ionizable residues on the surface of other carbonic anhydrase molecules in solution. Such a possibility is unlikely due to the sub-micromolar concentrations of enzyme used in all of our experiments.

The data of Table 1 indicate that K91 and Y131 make substantial contributions to proton transfer during hydration, but their replacement still leaves considerable activity, near 3×10^4 s^{-1} at pH near 9 for the quadruple mutant of Table 1, which indicates that there remain other proton shuttle residues. Although this is a high rate of catalysis, it is pertinent that proton transfer to hydroxide in solution could be close to this value; $k_2[OH^-] \cong (10^9\ M^{-1}\ s^{-1}) \times (10^{-5}\ M) = 10^4\ s^{-1}$ at this pH, where k_2 is a roughly estimated diffusion-controlled bimolecular rate constant for hydroxide ion encounter with carbonic anhydrase perhaps similar to that found for cyanide (*22*). Although hydroxide might contribute as a proton acceptor, the observation of a plateau in k_{cat} at high pH (Figure 3) indicates that hydroxide is not the main proton acceptor at pH up to 9. The results indicate that the predominant proton shuttle residues, but not all of the proton shuttle residues, have been accounted for in mCA V. That the remaining catalytic activity in CO_2 hydration of our least active mutants of Table 1 still have a pK_a of k_{cat} near 9 indicates that the remaining proton shuttles are likely basic residues such as Tyr 58 or perhaps Lys 133 or even more distant basic groups. These more basic groups are likely to have a thermodynamic advantage as proton acceptors as compared with histidine residues of expected pK_a near 6 or 7; besides, the crystal structure of the truncated form of mCA V used in these studies shows no histidine residues near the mouth of the active-site cavity (*3*). There is a further argument that the proton acceptors unaccounted for lie on the surface of the enzyme rather deeper than in the active-site cavity. That addition of the buffer Ted caused no enhancement of R_{H_2O}/[E] catalyzed by Y64A/K91A/Y131A mCA V indicates that this bulky buffer cannot enter the active-site cavity to transfer a proton to the zinc-bound hydroxide—the catalysis is sustained by the various surrounding proton donors (and water) that are at their equilibrium protonation states in this isotope exchange at chemical equilibrium. However, Ted caused a very large increase in the initial velocity of catalyzed CO_2 hydration, suggesting that it can accept protons from proton shuttle sites closer to or on the surface of the enzyme.

Although in single mutants these sites had small change as compared with wild type, the multiple mutants Y64A/K91A/Y131A and Y64A/K91A/Y131A/K132A had values

[2] Earnhardt, J. N., Wright, S. K., Qian, M. Z., Tu, C. K., Laipis, P. J., Viola, R. E., and Silverman, D. N., manuscript in preparation.

of k_{cat} reduced to 22% and 10% of that of wild type while showing no substantial decrease in k_{cat}/K_m (Table 1). Ignoring uncertainties in k_{cat} in Table 1, these percentages represent a simple additive effect of the replacements of Y64 and K132 beyond that of the double mutant K91A/Y131A. This suggests that we have accounted for the most significant proton shuttles of mCA V and emphasizes our observation that there is no single prominent shuttle as in HCA II, but that a group of residues near the rim of the active-site cavity each make a relatively small contribution to the proton transfer to solution.

The interaction between Lys 91 and Tyr 131 in the catalytic pathway is clearly not additive as indicated by comparison of k_{cat} for these single mutants and the double mutant K91A/Y131A (Table 1). That is, these residues are not acting independently in their role supporting proton transfer. Rather the double mutant causes no additional decrease in catalysis beyond either of the single mutants. This is a form of antagonism, as described by Mildvan et al. (*23*), between two residues that becomes evident upon observing catalysis by the double mutant. Two possible explanations account for this antagonistic effect: (i) The side chains of Lys 91 and Tyr 131 are adjacent to one another at the mouth of the active site cavity (Figure 1). These two residues form a proton transfer chain in which both are required sequentially to transfer protons out to solution. (ii) The antagonistic effect could be structural in which one residue is restricting the mobility of the second to conformations in which proton transfer occurs.

As anticipated, this effect of basic residues is not specific for mCA V. The pH profiles of k_{cat} for at least five of the seven functional isozymes in the α class (CA II, III, IV, V, and VII) demonstrate a dependence on ionizations at high pH that cannot be attributed to His 64. For human CA II, this is demonstrated in H64A.[3] In human CA III, there is an increment in k_{cat} of unknown source observed at pH > 8 (see Figure 2 of Jewell et al.; *12*). Murine CA IV wild type has a pH dependence of k_{cat} described by two ionizations, and in the H64A mutant the groups with pK_a near 9 remain (see Figure 6 of Hurt et al.; *24*). Finally, the murine form of isozyme VII has a pH dependence for k_{cat} described by two ionizations, one of which is assumed to be the histidine at position 64 and the other at higher pH is proposed to be another active site residue ionizing at high pH).[4] It is possible to consider this common observation for many isozymes of carbonic anhydrase as due to an accumulation of basic amino acids occurring near the active-site cavity in many of these isozymes; for example, CA II, III, IV, V, and VII all contain a lysine at positions 169/170 as well as other lysines and tyrosines located at the mouth of the active site cavity. Thus we conclude that in mCA V and likely in other isozymes of the α class of the carbonic anhydrases there are multiple proton transfers contributing to the overall catalytic efficiency of catalysis.

[3] Earnhardt, J. N., Qian, M. Z., Tu, C. K., Laipis, P. J., and Silverman, D. N., unpublished observations.

[4] Earnhardt, J. N., Qian, M. Z., Tu, C. K., Lakkis, M. M., Bergenhem, N. C. H., Tashian, R. E., Laipis, P. J., and Silverman, D. N. (1998) manuscript in preparation.

ACKNOWLEDGMENT

We thank Bret Schipper for excellent technical assistance.

REFERENCES

1. Dodgson, S. J. (1991) in *The Carbonic Anhydrases* (Dodgson, S. J., Tashian, R. E., Gros, G., Carter, N. D., Eds.) pp 297−306, Plenum Press, New York.
2. Heck, R. W., Tanhauser, S. M., Manda, R., Tu, C. K., Laipis, P. J., and Silverman, D. N. (1994) *J. Biol. Chem. 269*, 24742−24746.
3. Boriack-Sjodin, P. A., Heck, R. W., Laipis, P. J., Silverman, D. N., and Christianson, D. W. (1995) *Proc. Natl. Acad. Sci. U.S.A. 92*, 10949−10953.
4. Lindskog, S. (1997) *Pharm. Ther. 74*, 1−20.
5. Steiner, H., Jonsson, B. H., and Lindskog, S. (1975) *Eur. J. Biochem. 59*, 253−259.
6. Tu, C. K., Silverman, D. N., Forsman, C., Jonsson, B. H., and Lindskog, S. (1989) *Biochemistry 28*, 7913−7918.
7. Eriksson, A. E., Kylsten, P. M., Jones, T. A., and Liljas, A. (1988) *Protein Struct. Funct. Genet. 4*, 283−293.
8. Heck, R. W., Boriack-Sjodin, P. A., Qian, M. Z., Tu, C. K., Christianson, D. W., Laipis, P. J., and Silverman, D. N. (1996) *Biochemistry 35*, 11605−11611.
9. Silverman, D. N., and Lindskog, S. (1988) *Acc. Chem. Res. 21*, 30−36.
10. Liang, Z., Jonsson, B. H., and Lindskog, S. (1993) *Biochim. Biophys. Acta 1203*, 142−146.
11. Ren, X., Tu, C. K., Laipis, P. J., and Silverman, D. N. (1995) *Biochemistry 34*, 8492−8498.
12. Jewell, D. A., Tu, C. K., Paranawithana, S. R., Tanhauser, S. M., LoGrasso, P. V., Laipis, P. J., and Silverman, D. N. (1991) *Biochemistry 30*, 1484−1490.
13. Kunkel, T. A. (1985) *Proc. Natl. Acad. Sci. U.S.A. 82*, 488−492.
14. Tanhauser, S. M., Jewell, D. A., Tu, C. K., Silverman, D. N., and Laipis, P. J. (1992) *Gene 117*, 113−117.
15. Studier, F. W., Rosenberg, A. H., Dunn, J. J., and Dubendorff, J. W. (1990) *Methods Enzymol. 185*, 60−89.
16. Khalifah, R. G., Stader, D. J., Bryant, S. H., and Gibson, S. M. (1977) *Biochemistry 16*, 2241−2247.
17. Khalifah, R. G. (1971) *J. Biol. Chem. 246*, 2561−2573.
18. Silverman, D. N. (1982) *Methods Enzymol. 87*, 732−752.
19. Simonsson, I., Jonsson, B. H., and Lindskog, S. (1979) *Eur. J. Biochem. 93*, 409−417.
20. Jackman, J. E., Merz, K. M., and Fierke, C. A. (1996) *Biochemistry 35*, 16421−16428.
21. Scolnick, L. R., and Christianson, D. W. (1996) *Biochemistry 35*, 16429−16434.
22. Prabhananda, B. S., Rittger, E., and Grell, E. (1987) *Biophys. Chem. 26*, 217−224.
23. Mildvan, A. S., Weber, D. S., and Kuliopulos, A. (1992) *Arch. Biochem. Biophys. 294*, 327−340.
24. Hurt, J. D., Tu, C. K., Laipis, P. J., and Silverman, D. N. (1997) *J. Biol. Chem. 272*, 13512−13518.

BI9729209